Experimental Observation of Electrons Accelerated in Vacuum to Relativistic Energies by a High-Intensity Laser

G. Malka, E. Lefebvre, and J. L. Miquel

Commissariat à l'Energie Atomique, Limeil-Valenton, 94195 Villeneuve-Saint-Georges Cedex, France

(Received 25 October 1996)

Free electrons have been accelerated in vacuum to MeV energies by a high-intensity subpicosecond laser pulse (10^{19} W/cm^2, 300 fs). The experimental data are in good agreement with the relativistic motion of electrons in a spatially and temporally finite electromagnetic field, both in terms of maximum energy and scattering angle. [S0031-9007(97)02998-0]

PACS numbers: 41.75.Lx, 52.40.Nk, 52.75.Di

With the advent of the chirped pulse amplification technique [1], compact lasers can deliver multiterawatt short pulses, with focused intensities as high as 2×10^{19} W/cm^2 [2]. At this intensity, the electron classical oscillation velocity v_{osc} exceeds the speed of light in vacuum c. Indeed, the ratio of these velocities reads $a = v_{osc}/c = eE/m\omega_0 c = (I_{18}\lambda^2/1.37)^{1/2}$, where e is the electron charge, E is the magnitude of the laser field at focus, m is the electron mass, ω_0 is the laser angular frequency, I_{18} is the laser intensity in units of 10^{18} W/cm^2, and λ is the laser wavelength in μm. For a maximum intensity $I \approx 10^{19}$ W/cm^2, a reaches 3, defining an *ultrarelativistic regime*. The electric and magnetic fields at focus exceed 100 GV/cm and 300 MG, respectively. The ponderomotive potential of the electromagnetic wave is of the order of 1 MeV.

In this Letter, we present an experiment where free electrons are accelerated in vacuum directly by an intense subpicosecond laser pulse to MeV energies. Around the laser focus, the laser electric field makes electrons oscillate along the polarization direction, and simultaneously accelerates them along the propagation direction by the $\mathbf{v} \times \mathbf{B}$ force. In the focal region, the electrons will sample very different field amplitudes and can be scattered out of the pulse envelope in a few laser periods [3]. This so-called high-intensity ponderomotive scattering [3] is then a generalization to the high-irradiance regime of the usual ponderomotive acceleration.

The latter has already been observed—at low intensity, accelerating electrons by a fraction of an eV [4] or a few keV [5], and a high intensity, about 100 keV [6] for electrons initially at rest. The interaction of the laser pulse with electrons can be explained from two complementary points of view: In the corpuscular (quantum) theory, it is usual to define the Compton scattering multiphoton interaction [6], which corresponds to the absorption of several photons at ω_0 by one electron, accompanied by the emission of a single photon. In wave theory, the interaction is described by electrons and the electromagnetic field [3]. We choose to use this latter point of view to explain our experiments, because it easily gives the relations between initial and final electron energies, the laser intensity and its shape, and the electron scattering angle [3]. The electron dynamics is governed by the relativistic equation of motion for an electron interacting with an electromagnetic field.

An order of magnitude for the energies that we can expect is given by the maximum energy that the electrons would reach if the laser wave were plane (e.g., transversely infinite). It approximately reads [3] $\gamma_{max} \approx \gamma_0[1 + (a^2/2)(1 + v_0/c)]$, where γ_0 and v_0 are the initial electron Lorentz factor and velocity, respectively. For our parameters, $\gamma_{max} \approx 2.7$ MeV. As we will see below, numerical simulation accounting for the temporally and spatially finite shape of our laser pulse cuts that first estimate down to 1.0 MeV, close to our experimental result.

The experiment described here is performed with the 80 TW P102 laser system [2] at CEA/LV (Fig. 1). First, keV electrons are created by the interaction of a nanosecond pulse with a 3000 Å thin plastic target, 6 mm away from chamber center. The so-called creation laser beam (one part of the noncompressed laser pulse: $\lambda = 1.056$ μm, pulse width of 750 ps) is focused by a $f/8$ lens onto the plastic target with a 10^{12}–10^{13} W/cm^2 intensity (1–

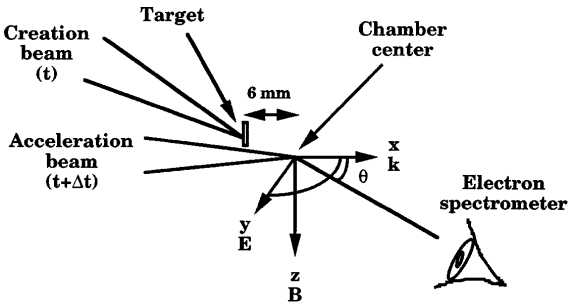

FIG. 1. Experimental setup. The creation beam parameters are 750 ps FWHM, $\lambda = 1.056$ μm, $I \approx 10^{12}$–10^{13} W/cm^2. The interaction beam parameters are $\lambda = 1.056$ μm, 300–500 fs FWHM, $I \approx 10^{19}$ W/cm^2 ($a \approx 3$), and $I \approx 5 \times 10^{18}$ W/cm^2 ($a \approx 2$) (focal spot of 10 μm diameter). Electrons are created by focusing the creation beam onto a 3000 Å thin foil plastic target. 6 mm farther, the interaction beam meets the electrons near its focus, with a delay of $\Delta t \approx 500$ ps. Observation angles are $\theta = 39°$ and $\theta = 46°$.

 0031-9007/97/78(17)/3314(4)$10.00

2 joules contained in a 50 μm focal spot diameter). Suprathermal electrons are expelled by Raman instability in a Boltzmann-like distribution of a few tens of keV [7]. We estimate that several 10^{12} fast electrons are going out of the plasma (assuming that 1% of the plasma electrons are accelerated by the Raman instability [7]). Five hundred picoseconds after the creation beam, which is the time for keV electrons to arrive near the chamber center, the high-intensity laser beam is focused at the chamber center with a $f/3$ on-axis parabola (interaction beam: $\lambda = 1.056$ μm, energy up to 20 J, pulse width $\tau = 300-500$ fs, 10 μm focal spot diameter, intensity up to 10^{19} W/cm^2).

We use successively two electron mass spectrometers to detect the accelerated particles [8]. A permanent and uniform magnetic field $B = 1700$ or 1000 G is created by a pair of magnets. A 10 μm Al thin foil protects the entrance of the spectrometer (7 mm diameter) against the light. Deflected electrons are detected by six thick silicon diodes. The spectral range is from 0.4 to 2.9 MeV ($B = 1700$ G), by a step of 0.5 MeV, with a width of 0.2 MeV. For $B = 1000$ G, the spectral range is from 0.2 to 1.3 MeV. The spectrometers are set at 39° and 46° of the laser propagation direction in the forward direction, in the horizontal plane, and at 15 cm from the chamber center. The laser polarization is horizontal, and the spectrometers are set in the $(\mathbf{E}, \mathbf{k})$ plane.

Figure 2 shows the spectra of accelerated electrons recorded with the two spectrometers for different shots. Laser intensities are $I \approx 10^{19}$ W/cm^2 ($a \approx 3$) for $\theta = 39°$ and $\theta = 46°$, and $I \approx 5 \times 10^{18}$ W/cm^2 ($a \approx 2$) for $\theta = 46°$. The maximum energy measured for these three different cases is $W_{\max} = 0.9 \pm 0.1$ MeV ($a = 3$, $\theta = 39°$), 0.63 ± 0.05 MeV ($a = 3$, $\theta = 46°$), and 0.63 ± 0.05 MeV ($a = 2$, $\theta = 46°$). Electrons with energies less than the maximum energies are also detected for these three cases. For each case, more than 10^5 electrons by

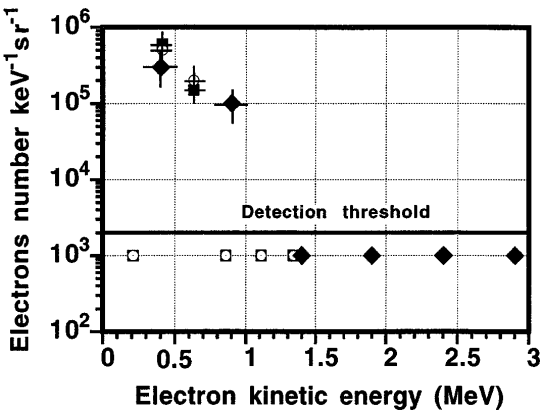

FIG. 2. Electron measurements recorded by the spectrometer at $\theta = 39°$ and $\theta = 46°$ for $a = 3$ and $a = 2$. The laser polarization is horizontal. The maximum energy is $W_{\max} = 0.9 \pm 0.1$ MeV ($a = 3$, $\theta = 39°$, diamonds), 0.63 ± 0.05 MeV ($a = 3$, $\theta = 46°$, circles), and 0.63 ± 0.05 MeV ($a = 2$, $\theta = 46°$, squares).

units of keV and sr are detected by the spectrometer. For $a = 2$ and $\theta = 39°$, we do not measure any signal.

To ascertain the validity of our results, we make different null tests: (i) Interaction beam only. (ii) Creation beam only. (iii) Both beams without target. (iv) By changing the polarization (horizontal to vertical). Since the spectrometer is in the horizontal plane, electrons are ejected horizontally and detected for horizontal polarization, whereas they are ejected vertically and not detected when the polarization is changed to vertical. (v) Spectrometer tests [8]—by inverting the magnetic field of the spectrometer or by putting a piece of glass in front of the spectrometer. In all these cases, we detect only a weak noise level (a few millivolts). We can then rule out laser-plasma interactions or important noises as a source of the electron signal (a few volts in the experiment).

Because of the extremely low density of electrons, collective effects can be neglected, and each electron behaves independently in the imposed electromagnetic field of the laser. We solved the corresponding equation of motion $m d_t(\gamma \mathbf{v}) = -e(\mathbf{E} + \mathbf{v} \times \mathbf{B})$ for a spatially and temporally finite, linearly polarized electromagnetic wave using a paraxial approximation for the fields [3]:

$$E_y = a \frac{mc\omega_0}{e} \frac{\exp[-y^2/w^2(x)]}{w(x)/w_0} f(\varphi) \times \sin\left[\varphi + \frac{k_0 y^2}{2R(x)} - \arctan\left(\frac{x}{x_R}\right)\right], \quad (1)$$

$$B_z = \frac{E_y}{c},$$

where $x_R = \pi w_0^2/\lambda_0$ is the Rayleigh length of the beam, $w(x) = w_0[1 + (x/x_R)^2]$ and $R(x) = x + x_R^2/x$ are, respectively, its characteristic width and its radius of curvature, both depending on position x along the propagation axis (negative before focus), φ is the phase, and $f(\varphi)$ the phase shape of the pulse. x is the laser propagation direction, y the electric field direction, and z the magnetic field direction. This equation is solved for $\lambda_0 = 1$ μm, $w_0 = 10$ μm, and taking for $f(\varphi)$ a sine-squared shape of total width 800 fs (300 fs FWHM in intensity).

With these two fields, it is possible to describe the electron motion with a good approximation during and after its interaction with the pulse. An electron that is initially in the plane containing the laser axis and the direction of polarization will remain in that plane. In that sense, a 2D model is enough. The transverse motion of the electron is governed by E_y, while the coupling of this transverse velocity with B_z will change the longitudinal momentum of the particle. We have calculated the longitudinal field E_x arising from focalization of the beam, and found that it is always one order of magnitude smaller than the incident field. As a consequence, and since the high-intensity interaction with the electron only lasts a very short time, the longitudinal field has been neglected in our calculations.

At relativistic irradiance, the standard small-amplitude approximation that leads to the concept of ponderomotive scattering can no longer be made. However, it is still adequate to visualize the electron as "surfing" on the time- and space-varying pulse envelope along the laser axis, and being eventually scattered down the wings of the pulse, where the irradiance is lower. The acceleration is only made possible by the finite transverse extent of the pulse: If it were transversely infinite, plane-wave results would apply and result in zero net acceleration. The electron energy gain will hence be related to the spatiotemporal profile of the laser pulse. From the above discussion, it is clear that scattering will only occur in the $(\mathbf{E}, \mathbf{k})$ plane.

Figure 3 shows the energy and angle in the $(\mathbf{E}, \mathbf{k})$ plane of the electrons scattered by the laser pulse for a laser amplitude $a = 3$ ($I\lambda^2 = 1.2 \times 10^{19}$ W μm^2/cm^2). They both depend on x_0, the position along the propagation axis at which the particle is overtaken by the pulse. Two curves have been computed for electrons with initial longitudinal velocities $v_0 = 0.1c$ (2.5 keV) and $v_0 = 0.2c$ (10 keV). The maximum kinetic energy is obtained for the electrons that meet the laser a few tens of micrometers before focus. For $v_0 = 0.1c$ (2.5 keV), the maximum energy is $W_{\max} \approx 0.95$ MeV ($\gamma \approx 2.9$), and, for $v_0 = 0.2c$ (10 keV), $W_{\max} \approx 1$ MeV ($\gamma \approx 3.0$). Maximum energy gain corresponds to a local minimum of the angular deflection, at $\theta = 43.1°$ for $v_0 = 0.1c$ and at $\theta = 39.8°$ for $v_0 = 0.2c$. For a lower gain, the angle opens. At the maximum scattering angle, the energy gain is already quite low: $\theta_{\max} \approx 65°$ and $W_{\max} \approx 0.05$ MeV ($\gamma = 1.1$) for $v_0 = 0.1c$, and $\theta_{\max} \approx 55°$ and $W_{\max} \approx 0.1$ MeV ($\gamma = 1.2$) for $v_0 = 0.2c$. The gain decreases further as the angle drops to zero, corresponding to electrons whose trajectories have only been slightly perturbed by the pulse.

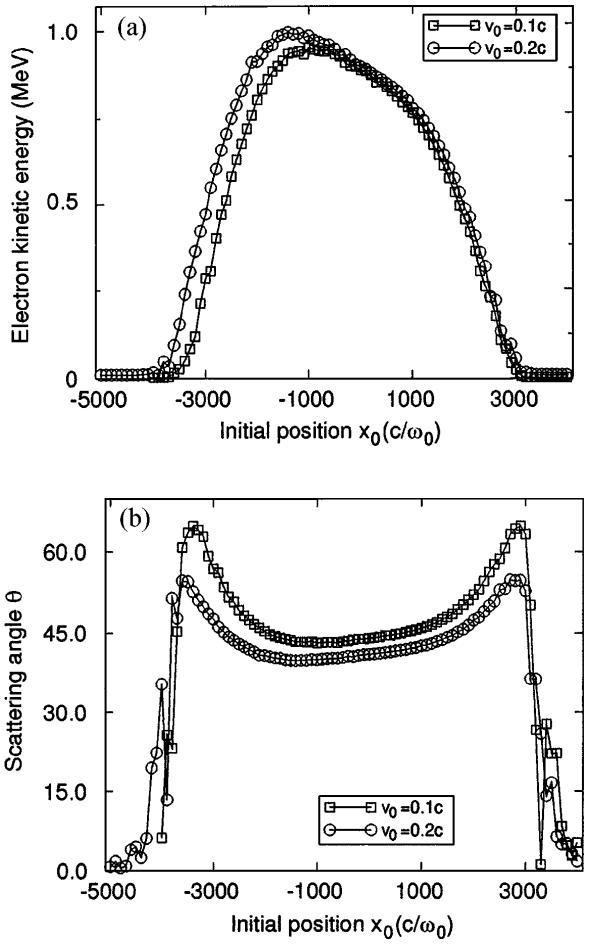

FIG. 3. Electron kinetic energy (a) and scattering angle θ (b) as a function of the electron injection position x_0 for $a = 3$. The position is counted in units of c/ω_0 ($2\pi c/\omega_0 = \lambda = 1.056$ μm). Initial energies are $W_0 = 2.5$ keV and $W_0 = 10$ keV, corresponding to velocities in the propagation direction (x axis) $v_0 = 0.1c$ and $v_0 = 0.2c$, respectively. Laser pulse duration is 300 fs FWHM, with a waist at focus $w_0 = 10$ μm.

The strong correlation between final energy γ and scattering angle θ is clearly apparent when we plot the simulation results on a polar diagram (W, θ). They show an excellent agreement with the theoretical law [3]:

$$\theta(\gamma) \approx \arctan\left(\frac{\sqrt{2(\gamma/\gamma_0 - 1)/(1 + \beta_0)}}{\gamma - \gamma_0(1 - \beta_0)}\right). \qquad (2)$$

The curves corresponding to Eq. (2) are delineated in Fig. 4 for some typical initial velocities (for the sake of clarity, simulation results of Fig. 3 have not been plotted on those curves). It is worth noting that Eq. (2), stemming from energy and momentum transfer in the photon field, does not involve the laser pulse parameters (temporal and spatial profiles, and maximum field). These parameters only govern the maximum energy that can be reached by the scattered electrons. This maximum-energy limit is plotted with closed symbols in Fig. 4 for $a = 3$ and $a = 2$. Using this polar representation, it is straightforward to see that, for a given ejection angle, the spectrometer collects

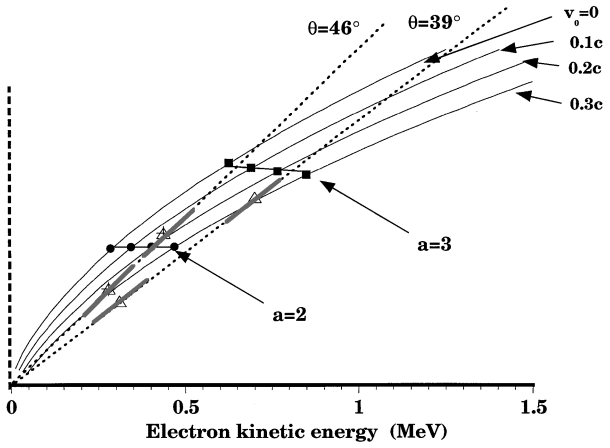

FIG. 4. Polar diagram: electron kinetic energy as a function of scattering angle θ. The four solid curves are the theoretical formula Eq. (2) for different initial velocities v_0. The closed symbols represent the maximum computed energies for the same initial velocities and two laser irradiances: $a = 2$ (circles) and $a = 3$ (squares). The dashed lines indicate the experimental angles of sight: $\theta = 39°$ and $\theta = 46°$.

electrons with different initial velocities that have been accelerated to different final energies. The two dashed radii drawn on Fig. 4 correspond to the experimental angles of sight, $\theta = 39°$ and $\theta = 46°$. When we follow these radii up to the $a = 2$ or $a = 3$ limits, we can make the following predictions: (i) For $\theta = 39°$ and $a = 2$, only electrons with initial velocity greater than $0.3c$ can be detected—we thus expect a very low signal. (ii) For $\theta = 39°$ and $a = 3$, the maximum kinetic energy should be 1.0 MeV, and not much signal is expected below 0.8 MeV. (iii) For $\theta = 46°$ and $a = 2$, the maximum energy should be 0.6 MeV. (iv) For $\theta = 46°$ and $a = 3$, it should be 0.8 MeV for particles with initial velocity above $0.05c$.

Despite the crude description of the pulse temporal variations, we find that our numerical results are in good agreement with the experiments. For $\theta = 39°$ and $a = 2$, no signal is detected, as expected. For $(\theta = 46°, a = 2)$ and for $(\theta = 39°, a = 3)$, there is good agreement between the experimental and theoretical maximum energies. For the $(\theta = 46°, a = 3)$ case, the measured maximum energy is slightly lower than predicted: 0.63 MeV instead of 0.8. In fact, the theoretical value falls in the energy range between two consecutive diodes of the spectrometer, and cannot therefore be detected. On the other hand, in the $(\theta = 39°, a = 3)$ case, no signal is expected below 0.8 MeV, contrary to what is observed. The reason for this lower energy component is still unclear to us.

An effective length of approximately 800 μm is obtained in Fig. 2 by requesting that $W > 400$ KeV. Similarly, we have calculated that the transverse effective area for the process is around $3 \times 3\ \mu\text{m}^2$. The volume where free electrons and photons can interact is then at least equal to 10^{-8} cm^3. In comparison, the volume over which the 10^{12} keV electrons are spread by Raman instability is roughly 0.1 cm^3 (assuming emission in 1 sr). The number of electrons that can interact with the pulse is then of the order of 10^5 per shot. In comparison, the detected signal is 10^5 electrons by keV and sr, e.g., a few 10^4 electrons measured per shot.

In summary, we observed the relativistic acceleration to MeV kinetic energy of free electrons in vacuum by the Lorentz force of an ultraintense laser beam. The experimental results are in good agreement with the computation of the electron trajectories in the laser field. This proof-of-principle experiment can be improved to accelerate electrons to much higher energy, because the gain is quite large—in a^2 [3] instead of a [8,9] for generation at a vacuum-plasma interface. From another point of view, with an improved spectral width of the spectrometer, we could have an indirect way to measure the laser electric field at focus.

We thank F. Amiranoff, L. Bergé, G. Bonnaud, B. Canaud, D. Juraszek, and M. Louis-Jacquet for fruitful discussions. We wish to acknowledge encouragement and support from S. Jacquemot and A. Jolas, the technical assistance of the P102 staff at CEA Limeil (I. Allais, N. Blanchot, E. Mazataud, and A. Pierre), as well as R. Caland for target fabrication.

[1] D. Strickland and G. Mourou, Opt. Commun. **56**, 219 (1985).
[2] N. Blanchot *et al.*, Opt. Lett. **20**, 395 (1995); C. Rouyer *et al.*, Opt. Lett. **13**, 55 (1995).
[3] F. V. Hartemann *et al.*, Phys. Rev. E **51**, 4833 (1995).
[4] Ph. Bucksbaum, M. Bashkanski, and T. J. McIlrath, Phys. Rev. Lett. **58**, 349 (1987).
[5] P. Monot *et al.*, Phys. Rev. Lett. **70**, 1232 (1993).
[6] C. I. Moore, J. P. Knauer, and D. D. Meyerhofer, Phys. Rev. Lett. **74**, 2439 (1995); D. D. Meyerhofer, J. P. Knauer, S. J. Naught, and C. I. Moore, J. Opt. Soc. Am. B **13**, 113 (1996).
[7] C. Rousseaux *et al.*, Phys. Fluids B **4**, 2589 (1992).
[8] G. Malka and J. L. Miquel, Phys. Rev. Lett. **77**, 75 (1996).
[9] S. C. Wilks *et al.*, Phys. Rev. Lett. **69**, 1383 (1992).